



Valvular Heart Disease Assessment by CMR

18

Patrycja Z. Galazka and Raymond Y. Kwong

General Overview

Cardiovascular magnetic resonance (CMR) has unique capabilities which can greatly benefit the assessment of the patient with cardiac valve disease [1]. In the last 20 years, CMR has emerged as an alternative to noninvasive modality without ionizing radiation that is applicable in patients with valvular heart disease. Echocardiography remains the standard tool for the initial assessment of valvular pathology; however, it may be inconclusive in some patients at which time CMR might accurately answer the clinical question. CMR provides images of valve anatomy and allows qualitative and quantitative evaluation of stenosis and regurgitation. CMR can also confidently discern the consequences of particular valvular lesions, including the effects of ventricular volume or pressure overload and alternations in systolic function [2]. Furthermore, CMR is able to evaluate great vessel anatomy and the presence of the myocardial scar which can be of prognostic significance. Therefore, CMR's versatility in assessment of valvular heart disease can significantly guide the clinician and advance patient's care.

Valvular Anatomy

Although 2D echocardiography remains the primary imaging modality for visualization of valvular anatomy, the CMR also has potential to visualize all parts of the valve (leaflets, chordae tendineae, and papillary muscles) throughout the

entire cardiac cycle [2]. An important advantage of CMR is its ability to provide unlimited imaging planes tailored to individual anatomy [2, 3]. The most frequently used CMR pulse sequence to assess valve anatomy is steady-state free-precession (SSFP) sequence which is the workhorse of the CMR imaging. This sequence has excellent blood to myocardium contrast and a high intrinsic signal to noise ratio and has largely replaced gradient echo as the preferred pulse sequence for cine imaging of valve anatomy, although gradient-echo sequences also can be used to assess for valvular pathology when there is significant off resonance artifact.

The typical CMR study for evaluation of a valvular lesion involves performing a complete set of sequential short-axis (every 10 mm from base to apex) and long-axis (two-, three-, four-chamber views) cine images using the SSFP sequence depending on the valve of interest [4] (Fig. 18.1). To produce SSFP cine image throughout the systole and diastole, image acquisition is gated to ECG and occurs over several cardiac cycles and is obtained in a single breath-hold (over 6–12 s). The typical spatial resolution is 1.5–2.0 per pixel with 6 mm slice thickness, and using the ultrafast pulse sequence, temporal resolution of 25–35 ms (frame rates of 30–40 cm/s) can be achieved within 5–6 second breath-hold [4]. Spoiled gradient-echo sequences remain useful on occasions for visualizing the extent of flow disturbance in selected cases [1].

In addition to valvular anatomy such as evaluation of congenital abnormalities (bicuspid aortic valve, parachute mitral valve, aberrant papillary muscles, and chordal attachments), CMR can provide visualization of a cardiac valvular masses such as vegetations, thrombi, or tumors [2]. Non-cine pulse sequences, T1 weighted and T2 weighted based on gradient recalled echo or turbo spin-echo techniques with or without fat suppression, and segment recovery gradient may aid in tissue characterization of the masses as well as can be beneficial in assessment of extra-cardiac anatomy and thoracic vasculature [2, 5].

P. Z. Galazka

Non-invasive Cardiovascular Imaging, Cardiovascular Division,
Department of Medicine and Department of Radiology, Brigham
and Women's Hospital, Harvard Medical School,
Boston, MA, USA

R. Y. Kwong (✉)

Non-invasive Cardiovascular Imaging, Cardiovascular Division,
Department of Medicine, Brigham and Women's Hospital, Harvard
Medical School, Boston, MA, USA
e-mail: rykwong@bwh.harvard.edu

Flow and Velocity Quantification

The unique advantage of CMR is its direct ability to quantify flow using through-plane phase-contrast velocity mapping. In contrast to echocardiography or invasive catheterization techniques, flow quantification with CMR does not rely on geometric and mathematical assumptions [6]. For phase contrast, two opposing gradient pulses known as velocity encoding are added to the imaging sequence of pulses. In pixels containing static tissue, the effects of the two pulses cancel, but if the tissue moves in the time between the pulses, they leave a phase shift in that pixel accurately proportional to the velocity along the gradient's direction [7]. This net-phase shift can be displayed as a phase map with differences in signal intensity representing different velocities. Pixels depicting flow in the phase-encoding direction appear bright and opposite to phase-encoding direction appear dark. Objects with a phase-shift zero appear gray or speckled [2] (Fig. 18.2).

These images can be further enhanced with color-coding of the anterograde (red) and retrograde (blue) dynamic flow (Fig. 18.3).

Velocity mapping requires that the appropriate maximum encoding velocity (VENC) is programmed into the pulse sequence [2]. The VENC refers to the velocity that is encoded as the phase shift of 180 degrees and thus represents the maximum velocity that is displayed unambiguously on the velocity maps [5]. If the velocity phase shift exceeds 180 degrees range, it cannot be distinguished from one within +180 degree range, which is displayed instead known as velocity aliasing (wrap-around) [7]. The closer the programmed maximum velocity is to the maximum velocity present, the greater the sensitivity and accuracy of this technique to detect lower velocities within the region of interest [2]. As a compromise between high sensitivity and avoiding aliasing artifacts, it is recommended that the predicted peak velocity should cover approximately two-thirds of the interval set by the VENC [8]. Typical VENC's for normal aortic

Fig. 18.1 SSFP cine image of two-chamber image allows for excellent visualization of anterior mitral valve prolapse (arrow) (left) and an axial SSFP short-axis image of the mitral valve in diastole (right)

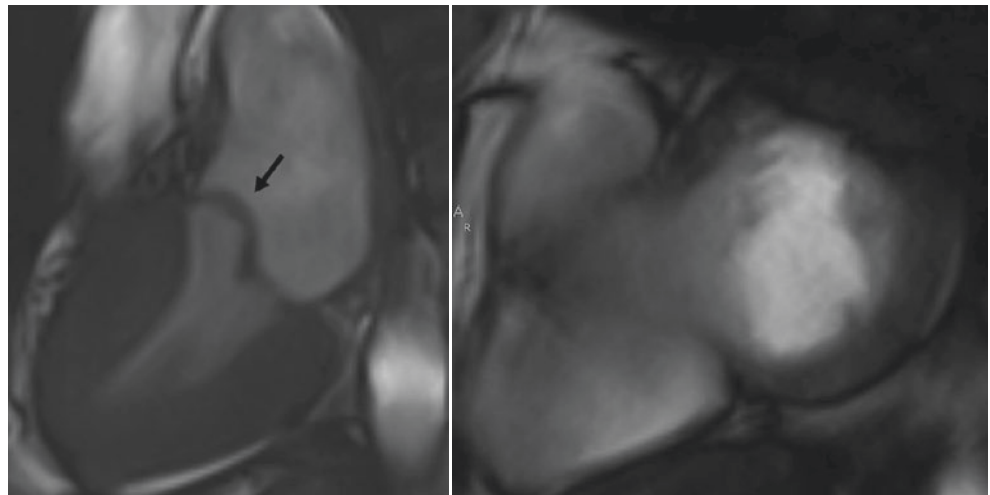
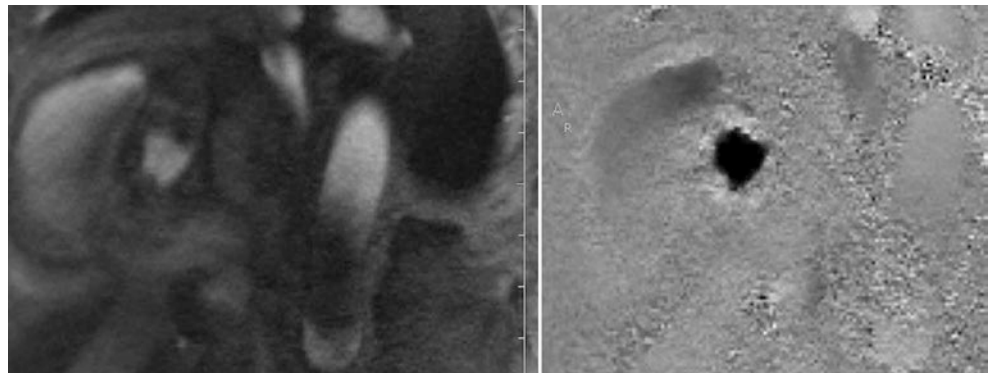


Fig. 18.2 Example of ECG-gated cine phase-contrast magnitude (right) and phase (left) images during systole at the normal functioning pulmonic valve level



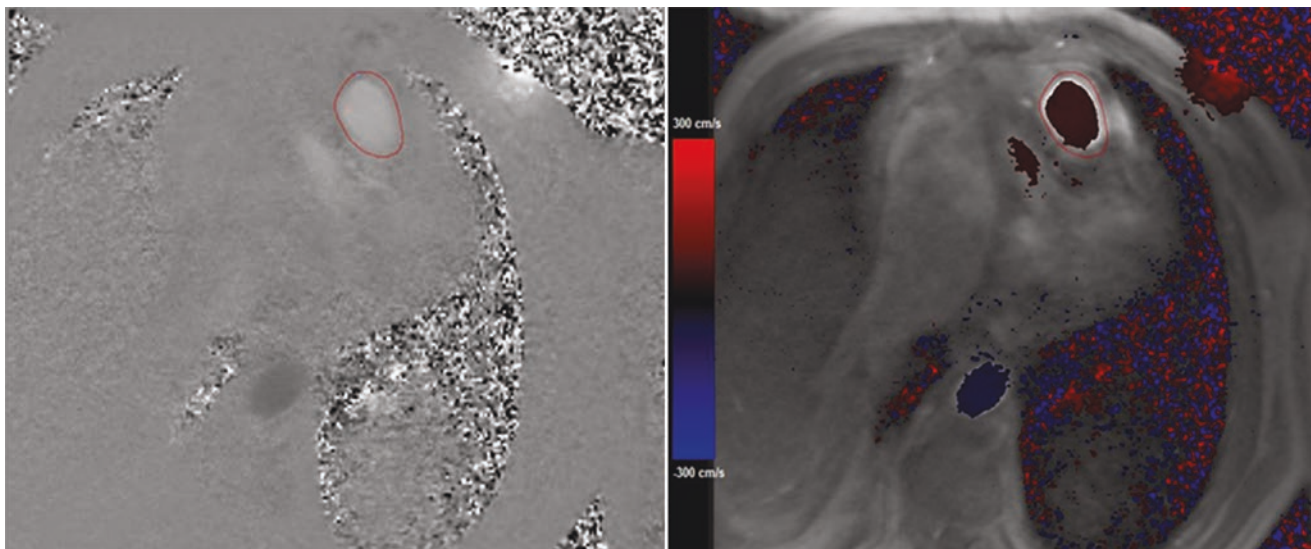


Fig. 18.3 Example of phase-contrast image at the level of pulmonary artery (left) and color-coded image (right) showing forward flow in the pulmonary artery and antegrade flow in the descending thoracic aorta

flow are in the region of 150 cm/sec increasing to 400 cm/sec or more for aortic stenosis [9]. The velocity mapping produces two sets of images: magnitude image and phase-velocity maps. The magnitude image is used for anatomic orientation of the imaging slice and to identify the boundaries of the vessel imaged [2]. The phase map encodes the velocities within each pixel. The uncontrolled phase errors must be removed to detect only the velocity-phase shift, so two scans typically “reference” and “velocity encoded” usually are acquired together. Subtracting the reference phase image from the velocity-encoded phase image makes the phase-contrast velocity map [7] (Fig. 18.4).

For “through-plane” velocity mapping, used for flow quantification, the operator should prescribe the image plane perpendicular to the direction of blood flow. Velocities can also be measured “in-plane” phase-contrast sequences, which measure velocities within the plane of the slice [6]. Ideally the in-plane sequences allow a long-axis visualization of the transvalvular jet and should be acquired before through-plane velocity mapping as they can demonstrate the origin and direction of the jet. This can be useful when planning subsequent perpendicular or through-plane slice [6]. The in-plane velocities are generally less accurate for measuring peak velocities especially in a stenotic valve due to partial volume effects, relatively low temporal resolution as compared to echocardiography, signal loss due to turbulence, and phase-shift errors [6]. The through-plane velocity mapping is a method of choice for assessing high-velocity jets. We in general obtain a stack of 3–5 parallel slices to ensure the data acquisition closest to the stenotic orifice, where maximum jet can be accurately assessed (Fig. 18.5).

Assessment of Ventricular Volumes, Function and Mass

Precise measurement of both left and right ventricular volumes, function and mass is very important for determining the impact of valve lesion on the ventricle [1]. It has been shown that both ventricular dilatation and reduced systolic function are poor prognostic indicators [10]. CMR is the most accurate and reproducible technique for assessing both right and left ventricular volumes and mass and is considered the gold standard [11–13]. The accuracy of CMR calculated volumes has been validated through both in vitro and in vivo methods [14]. Right ventricular volumes are especially difficult to assess with other modalities due to crescentic shape of the RV; therefore, CMR can be especially useful [1]. The technique that has won widespread acceptance is the short-axis multi-slice (multiple 2D or 3D) cine acquisition, where both ventricles are sampled from the atrioventricular ring to the apex, with subsequent planimetry of the endocardial and epicardial borders of the ventricles to derive the required volume and mass parameters [15]. During a breath-hold, a stack of 6–8 mm slices in SSFP sequence is obtained that covers the length of both ventricles. The ventricular volume is obtained from careful tracing endocardial borders in end-systolic and end-diastolic views which provide end-systolic and end-diastolic volumes from which stroke volume, cardiac output, and ejection fraction can be calculated [5]. Myocardial volume is the area occupied between the endocardial and epicardial border multiplied by the interslice distance. Similar to echocardiography, left ventricular mass is the product of this vol-

Fig. 18.4 Example of ECG-gated cine phase-contrast magnitude (right) and phase (left) images during systole at the normal functioning pulmonic valve level

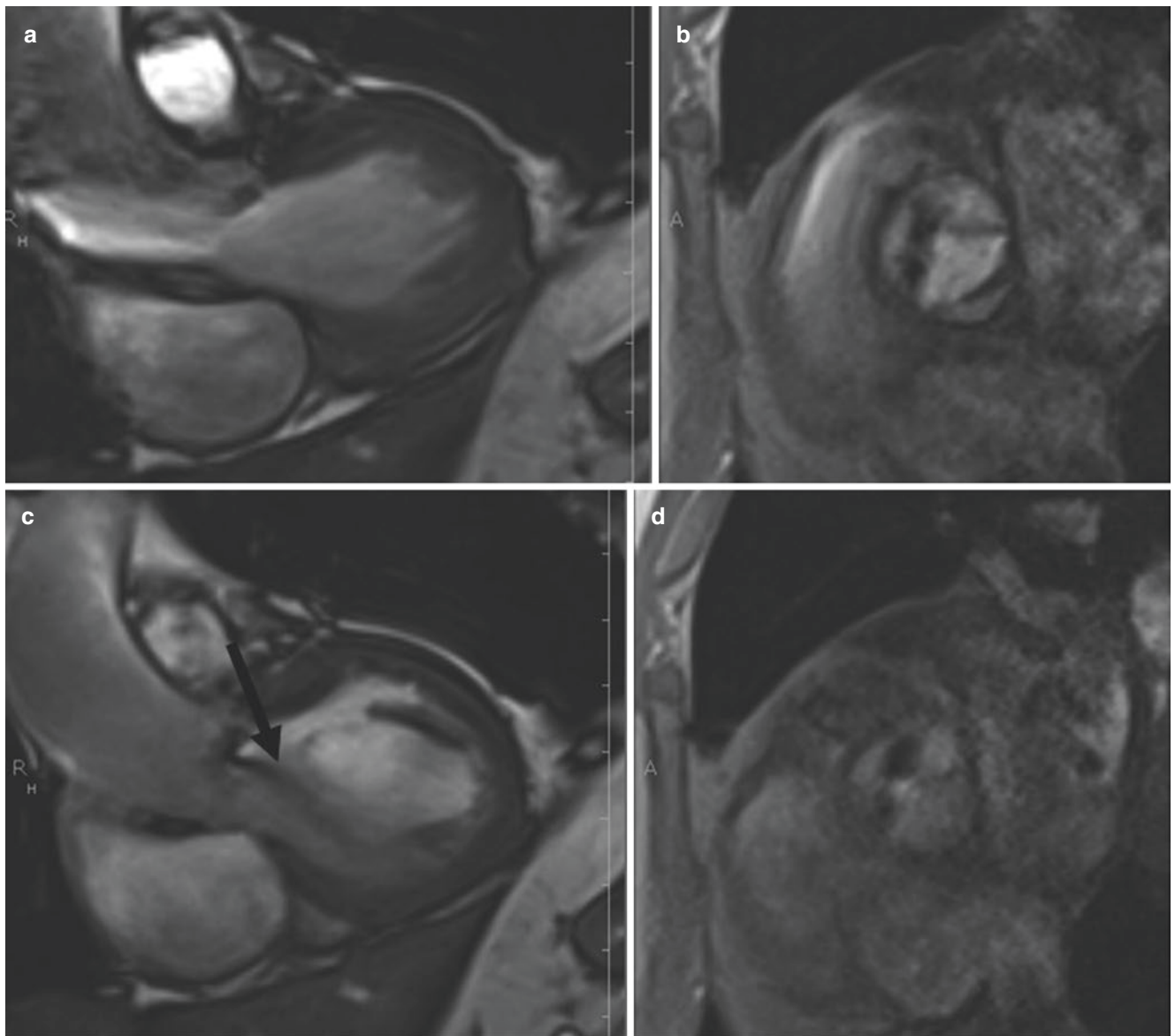
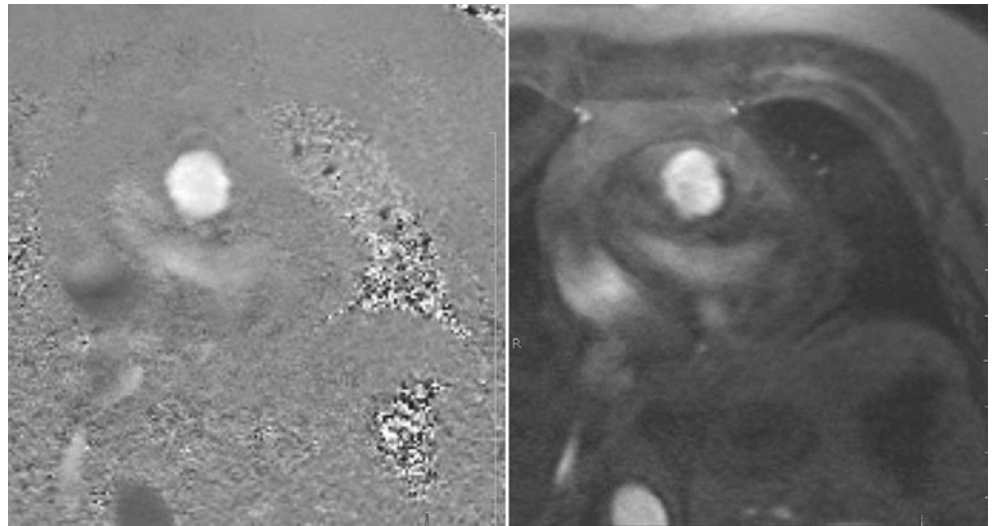


Fig. 18.5 SSFP cine left ventricular outflow oblique view image (a) in systole. This view allows to obtain a short-axis view at the aortic valve level which shows a bicuspid aortic valve in systole with right and left cusp fusion (b). From the short-axis view, through-plane velocity map-

ping can be planned out. Same views obtained in diastole showing aortic regurgitation (arrow) as a signal void in LVOT (c) and short-axis view at the aortic valve level which shows a bicuspid aortic valve in diastole (d)

ume and the density of the myocardium [16]. Papillary muscles and endocardial trabeculae should be excluded from the LV volume and included in the LV mass. LV mass is usually taken from the end-diastolic images [15].

Assessment of Aortic Stenosis

Aortic stenosis can be characterized by congenital or acquired impedance of blood flow from the left ventricle into the aorta and may be of subvalvular, supra-valvular, or most commonly of valvular etiology. Current guidelines by the American Heart Association/American College of Cardiology (AHA/ACC) recommend aortic valve surgery in virtually all symptomatic patients with severe aortic stenosis (Class I) and support surgical intervention for asymptomatic patients who demonstrated left ventricular systolic dysfunction or exertional hypotension (Class IIa) [10]. A CMR assessment of aortic stenosis can be enhanced with CMR through accurate assessment of the anatomy of the valve and the aortic root, precise quantification of the LV mass and function, and measurements of the velocity of the stenotic jet in instances when it is difficult to do with echo [1]. Similar to echocardiography, cardiac MRI allows for the assessment of aortic stenosis severity by use of two different approaches. One of them is direct planimetry by obtaining of the maximal anatomical orifice area using cine CMR imaging of the valve tips in systole [17, 18]. The excellent visualization of anatomy provided by SSFP cine short-axis image plane allows superb evaluation of severity of aortic stenosis with direct planimetry of the aortic valve orifice [19]. Second technique calculates functional orifice area by the continuity equation and the velocity time integrals obtained at the valve tips and through left ventricular outflow tract with phase-contrast imaging [20]. In contrast to echocardiography, the cross-sectional area of the left ventricular outflow tract (LVOT) can be directly measured without making geometric assumption. The continuity equation states that the flow at the LVOT level must equal the flow at the level of the aortic valve. Such measurement in CMR has been shown to have a high rate of intra- and inter-observer reproducibility [18, 21].

$$\text{Aortic Valve Area} = \frac{\text{LVOT velocity}}{\text{Aortic Valve velocity}} * \text{LVOT area}$$

After localization of the heart using three plane and oblique images, a three-chamber view and an oblique coronal breath-hold SSFP view cine should be prescribed where left ventricular outflow can be visualized well [22]. These are also optimal planes for identifying the signal void corresponding to the abnormal flow jet [23]. From these images, short-axis SSFP image is prescribed by placing the imaging plane through the aortic valve tips in systole. Free-breathing,

SSFP image slices should be thin (4–5 mm), and multiple slices parallel to the aortic valve opening should be acquired as they may aid in identifying the true valve orifice [1]. There is an excellent agreement between the planimetry of the aortic valve area using SSFP cine images and transesophageal echocardiography [17, 18, 20].

For the continuity equation, LVOT area, LVOT VTI, and AV VTI need to be assessed. One of the advantages of the CMR over echocardiography in continuity equation is ability to directly measure LVOT. Free-breathing, cine-gradient echo-segmented pulse sequences for through-plane phase-contrast imaging and velocity encoding should be acquired in the short-axis plane positioned just beyond the aortic leaflet tips and in the LVOT approximately 2 cm below the aortic annulus. The optimal short-axis slice position for measurement of peak transvalvular velocities is at the vena contracta just at or beyond the anatomic valve orifice in systole. In straight pipes with planar circular orifice plates, the vena contracta occurs about one orifice diameter downstream from the orifice [24]. The velocity encoding should be set in the through-plane direction at the maximal encoding velocity depending on severity of aortic stenosis (at least 4 m/sec in cases of severe aortic stenosis) for the transvalvular phase-contrast image and at least at 2.0 m/sec in the LVOT to avoid aliasing [22]. Due to small width of very high-velocity jets and partial volume effects, lower temporal resolution as compared to echocardiography, and artifacts from turbulent jets, the peak aortic velocity obtained by velocity mapping may be underestimated as compared to continuous wave Doppler obtained by echo [1]. Pressure gradient and valvular area measurements obtained with these imaging techniques have been shown to correlate accurately with data from cardiac catheterization and Doppler echocardiography [21].

Other advantages of CMR include ability to assess and differentiate between supra-valvular and subvalvular stenosis with accurate assessment of site of velocity acceleration with in-plane velocity mapping [1]. CMR can also accurately assess the diameter of the ascending aorta which is especially important in case of bicuspid aortic valves. Additionally, very accurate left ventricular mass assessment provides information regarding effect of aortic stenosis on the left ventricle [1]. Lastly, the presence of LGE which usually occurs patchy and mid-wall in the basal lateral wall indicating focal fibrosis or unrecognized infarct is an independent predictor of mortality in patients with AS undergoing AVR [25].

Assessment of Aortic Regurgitation

Per AHA/ACC 2014 Valvular guidelines, CMR is indicated in patients with moderate or severe aortic regurgitation (stages B, C, and D) and suboptimal echocardiographic images for the assessment of LV systolic function, systolic and diastolic volumes, and measurement of AR severity [10].

The severity of the aortic insufficiency can be semiquantitatively assessed by manually tracing the area and measuring the greatest length of the depicted signal void in left ventricle on cine imaging [26]. The signal void of the aortic regurgitant flow in diastole is best demonstrated by multi-planar imaging in the coronal plane centered on the LVOT and in the long axis of the left ventricle [27] (Fig. 18.6).

While this assessment of jet area ($r = 0.91$) and jet length ($r = 0.85$) is comparable to that of transesophageal echocardiography and provides a crude assessment of the severity of the regurgitant lesion, it cannot be overemphasized that the appearance of the signal void varies depending on the valvular abnormality, volume and pressure in the receiving cavity, and imaging parameters particularly the degree of dephasing allowed by the predefined TE [7, 28, 29]. The advantage of CMR in evaluation of aortic regurgitation is direct quantitative assessment of the degree of regurgitation and its consequences on LV volume and function which is especially important when serial measurements are required as per AHA/ACC guidelines; aortic valve replacement is supported in asymptomatic patients with severe left ventricular dilatation (>75 mm end-diastolic and >55 mm end-systolic echocardiographic diameters or LVEF $< 50\%$) [3, 30]. Myerson et al. showed that patients with aortic regurgitant fraction $>33\%$ quantified by CMR was associated with symptoms and progression to surgery [30].

CMR can accurately quantify the amount of regurgitation using through-plane phase-contrast velocity mapping from which derived values such as regurgitant fraction or regurgitant volume can be obtained. Flow can be measured by prescribing the imaging slice just above and below the aortic valve, quantifying both forward and regurgitant flow per cardiac cycle [31]. For forward flow, it is important to position the imaging plane just above the aortic valve as otherwise the velocity can be underestimated if it is placed in the ascending aorta [1]. Free-breathing, SSFP image slices should be thin (4–5 mm), and multiple slices above and below the aortic valve opening should be obtained. A magnitude image with the manually traced cross-sectional area of the valvular annulus is transferred to the corresponding phase image for each time frame. This enables measurement of the average velocity and provides the flow volume per heartbeat [32, 33].

$$\text{Regurgitant Fraction} = \frac{\text{Regurgitant Volume}}{\text{Forward Volume}}$$

It is also possible to calculate aortic regurgitation with ventricular volumes when a single-valve lesion such as aortic valve regurgitation is present. The regurgitant volume can be calculated from the difference of right ventricular and left ventricular stroke volumes using the modified Simpson method, in which the volumes of the ventricles are measured on a stack of parallel short-axis views [34].

$$SV(LV) - SV(RV) = \text{Aortic Valve Regurgitant Volume}$$

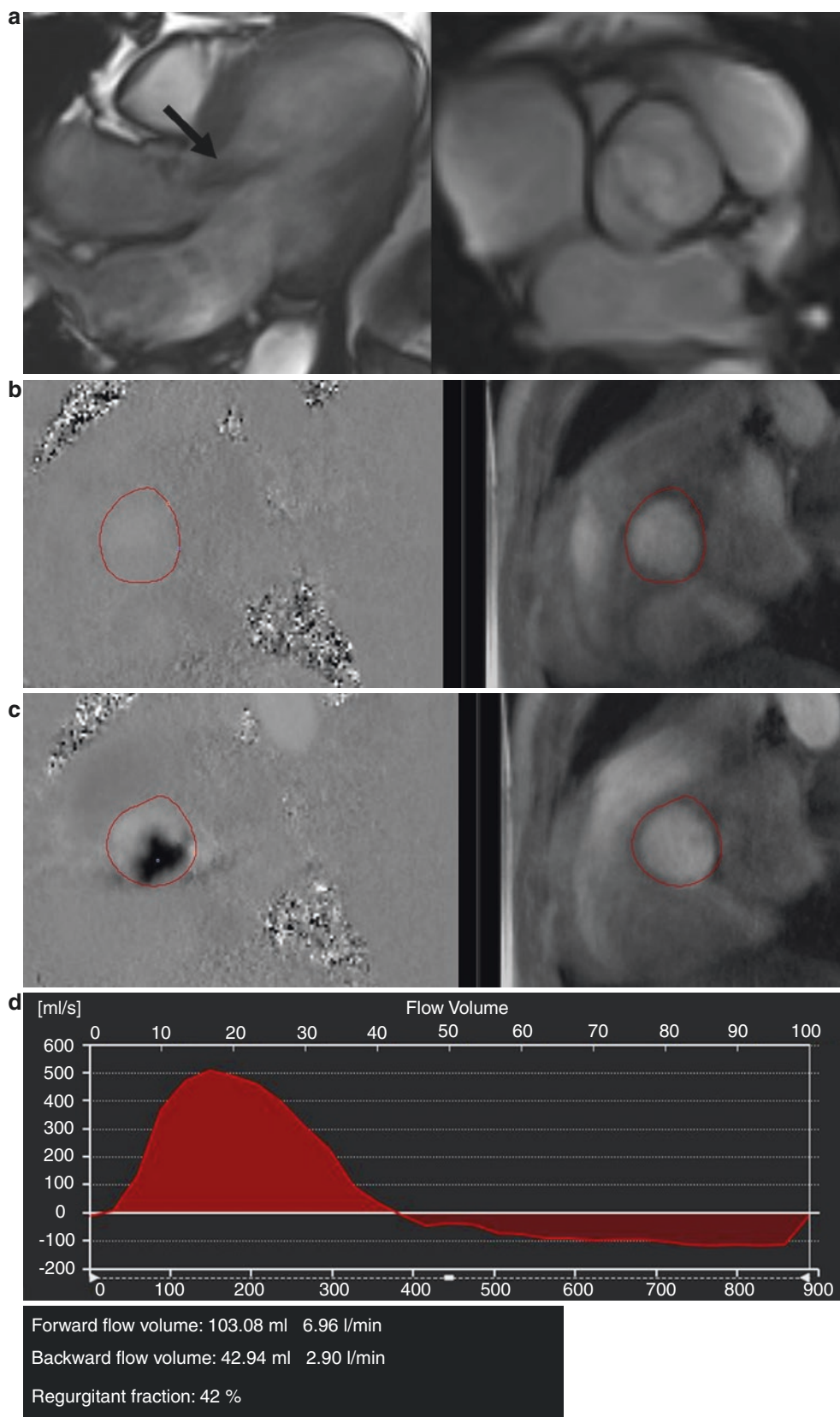
The measurement of regurgitant flow with phase contrast correlates well with the semiquantitative angiographic or echocardiographic grades of severity [31, 35]. The accuracy of aortic regurgitation quantification using CMR through-plane velocity mapping is also excellent when compared to in vitro studies [1].

Additionally, CMR also enables visualization of the aortic arch and may help determine the etiology of aortic regurgitation. For example, uniform dilatation of the aortic annulus and proximal ascending aorta is a finding that is compatible with aortoannular ectasia. Therefore, CMR allows for comprehensive assessment of the valve and its function as well as the aorta. Lastly, a new emerging technique of 4D flow CMR which refers to phase-contrast CMR with flow encoding in all three spatial directions that is resolved relative to all three dimensions of space and to the dimension of time along the cardiac cycle (3D + time = 4D) has been promising in estimating aortic regurgitation volume and fraction [27] (Fig. 18.7).

Assessment of Mitral Stenosis

Echocardiography, especially transesophageal echocardiography, remains the first-line technique for assessment of mitral stenosis, but cardiac MRI can be useful in selected cases of mitral stenosis as in patients with poor acoustic windows [1, 6]. Restriction in mitral valve opening during diastole results in mitral stenosis and produces a diastolic pressure gradient between the left atrium and left ventricle. As an alternative to echocardiography, CMR provides good visualization of the restricted leaflets and in particular an excellent visualization of the left ventricular outflow track [6]. Direct planimetry of the stenotic orifice can be performed in similar way as in the aortic stenosis. The imaging plane should be placed at the mitral valve tips in diastole [6]. Djavidani et al. showed that planimetry of the mitral valve by magnetic resonance imaging has good correlation with echocardiography although slightly overestimates MVA when compared to the PHT method by echocardiography and to invasive hemodynamics [36]. Diastolic flow and velocity also can be measured in this image plane with velocity-encoding cine magnetic resonance imaging which also shows good correlation with Doppler transthoracic echocardiography [37]. Velocity-encoded CMR can quantify MVA using the PHT method in a similar manner to that used in transthoracic echocardiography which is also comparable to a transthoracic echocardiography [38]. Atrial fibrillation in severe mitral stenosis can reduce the accuracy of flow measurements [6]. CMR also can be helpful in identifying LAA or LA thrombus especially in patients being considered for percutaneous mitral balloon commissurotomy [39].

Fig. 18.6 A 50-year-old male with history of bicuspid aortic valve. **(a)** SSFP cine three-chamber view showing eccentrically directed aortic regurgitation jet (arrow) (left) SSFP short axis at aortic valve level shows right and left coronary cusp fusion in a bicuspid valve (right). **(b)** Phase and magnitude images below the aortic valve shows forward aortic flow in black. **(c)** Phase and magnitude images obtained below the aortic valve shows regurgitant aortic flow in black. **(d)** Corresponding plots of velocity vs time-volume curve showing antegrade and retrograde flow with resultant regurgitation fraction of 42%



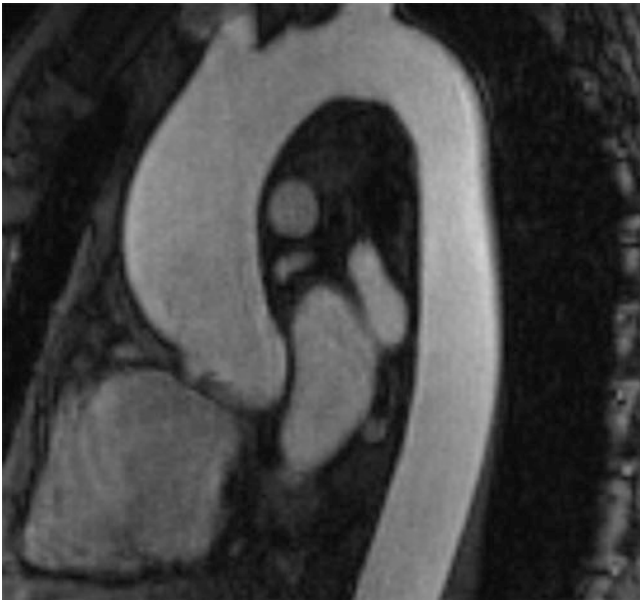


Fig. 18.7 MRA of dilated ascending thoracic aorta in a patient with bicuspid aortic valve

Mitral Regurgitation

Mitral regurgitation is caused by insufficiency of an abnormal mitral valvular apparatus that results in backward flow of blood from the left ventricle into the left atrium and produces an increase in total stroke volume. The AHA/ACC 2014 valvular guidelines recommend valve replacement in patients with severe mitral regurgitation with symptoms of congestive heart failure or left ventricular systolic dysfunction (LVEF 60%) and recommend the use of CMR to assess LV and RV size and function, as well as severity of MR, in situations where TTE is technically limited [10]. The main advantages of CMR over echocardiography are in quantitative assessment of both the regurgitation fraction as well as ventricular function and volume [1, 40]. In ischemic mitral regurgitation, CMR can also assess regional myocardial function and viability. Therefore, accurate assessment of severity of regurgitation, knowing the dysfunction responsible for it, the etiology of the condition, and LV size and function is very important.

An understanding anatomy of the mitral valve is very important for accurate imaging. CMR can assess mitral leaflets morphology and determine the etiology of the mitral regurgitation which has a very good agreement with transesophageal echocardiography. Multi-slice contiguous cines (5 mm slices) can be used for full evaluation of the mitral valve morphology and identification of prolapse and regurgitation of scallops which has correlated well with transesophageal echocardiography in patients prior to mitral repair [40]

Following standard two-, three-, and four-chamber long-axis views, a balanced SSFP end expiratory breath-hold cines, with ECG gating, and a short-axis stack (starting at the mitral annulus and continuing through the LV apex using 8 mm slice thickness) allow for accurate assessment of mitral anatomy [40]. From a basal short-axis image where mitral valve is well seen, a contiguous stack of oblique slices can be aligned orthogonal to the central line of the coaptation, oriented approximately parallel to the three-chamber LVOT long-axis plane. The stack of cines starts the superior (anterolateral) commissure adjacent to A1-P1 and progress toward the inferior (posteromedial) commissure adjacent to A3-P3 using a slice thickness of 5mm and interslice gap [40]. Additional orthogonal imaging slices are acquired through the commissures at each end of the mitral valve (A1-P1 and A3-P3) to better visualize these scallops. From the mitral stack and commissural images, each scallop of the mitral leaflet is well visualized, and the pathology can be delineated (Fig. 18.8).

Quantification of mitral regurgitation is usually performed with phase-contrast velocity mapping. First, aortic velocity mapping is performed in the ascending aorta above the sinotubular junction which is then subtracted from the left ventricular stroke volume in order to calculate mitral regurgitation volume which when divided by left ventricular stroke volume gives the regurgitant fraction [40].

$$\text{Mitral Regurgitant Volume (ml / beat)} = \text{LVSV} - \text{AoSV}$$

$$\text{Regurgitant Fraction} = \frac{(\text{MRV}) \times 100\%}{\text{LVSV}}$$

For quality control, the aortic forward volume should be within 5% of the pulmonary artery forward flow in the absence of intracardiac shunt [40]. And just as in the case of aortic regurgitation and the absence of other regurgitant lesions, MRV can also be calculated by subtracting RV stroke volume from LV stroke volume if there are no other regurgitant lesions.

$$\text{MRV} = \text{LVSV} - \text{RVSV}$$

The quantification of the mitral regurgitation correlates well with echocardiographic and angiographic assessment and has good reproducibility [41, 42]. The AHA/ACC 2014 valvular guidelines grade severe MR by echocardiography as regurgitant volume >60 ml and regurgitant fraction >50%. Myerson et al. followed 109 patients with CMR who had echocardiographic moderate to severe mitral regurgitation and showed that regurgitant volume >55 ml and regurgitant fraction >40% were associated with development of symptoms and need for surgery and showed better discriminatory ability than reference standard CMR-derived ventricular vol-

umes [43]. CMR should be considered in those patients when mitral regurgitation severity as assessed by echocardiography is influencing an important clinical decision, such as the decision to undergo surgery [44].

Pulmonary Stenosis

CMR is particularly valuable in assessment of pulmonary valve especially in congenital heart disease such as tetralogy of Fallot as it might be difficult to visualize the RVOT and the pulmonic valve with echocardiography due to its location immediately behind the sternum. Therefore, CMR should be considered as a gold standard for evaluation of the pulmonic

valve and RV outflow tract [1]. Balanced SSFP imaging of an oblique sagittal plane of RV outflow tract should be obtained which comprehensively includes the proximal pulmonary trunk and foreshortened view of right ventricle [1].

In order to visualize all three pulmonary leaflets, a double-oblique coronal plane is obtained along the pulmonary artery perpendicular to the valve. Then the plane through the now visible pulmonary cusps results in true short valvular axis [45].

A qualitative assessment of severity of pulmonary stenosis can be made from cine imaging by visualizing the valve motion and the stenotic jet [1]. As in the case of evaluation of mitral valve stenosis, direct planimetry of the valve orifice obtained in systole from the cine images at the valve tips is the preferred method for evaluating the severity [1]. Quantitative assessment

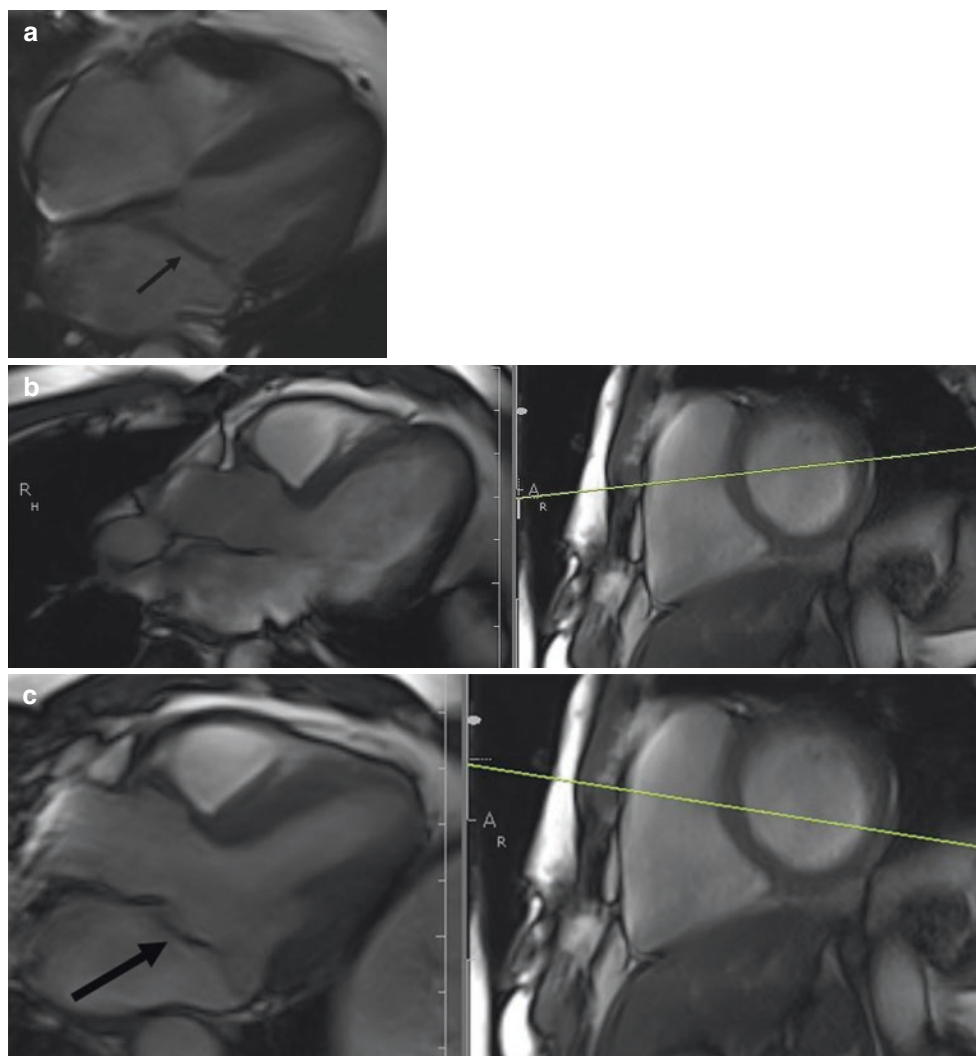


Fig. 18.8 A 50-year-old female with history of mitral regurgitation. (a) SSFP cine four-chamber view of anteriorly directed mitral regurgitation jet (arrow) seen in systole. (b) A1/P1 scallop assessment planned from the short-axis view at the mitral valve level. (c) A2/P2 scallop assessment planned from the short-axis view at the mitral valve level

showing anteriorly directed mitral regurgitation jet (arrow) originating from prolapsed P2 scallop. (d) A3/P3 scallop assessment from the short-axis view at the mitral valve level. (e) Magnitude (right) and phase (left) images at the mitral valve level in diastole. (f) Magnitude (right) and phase (left) images at the mitral valve level in systole showing mitral regurgitation in dark

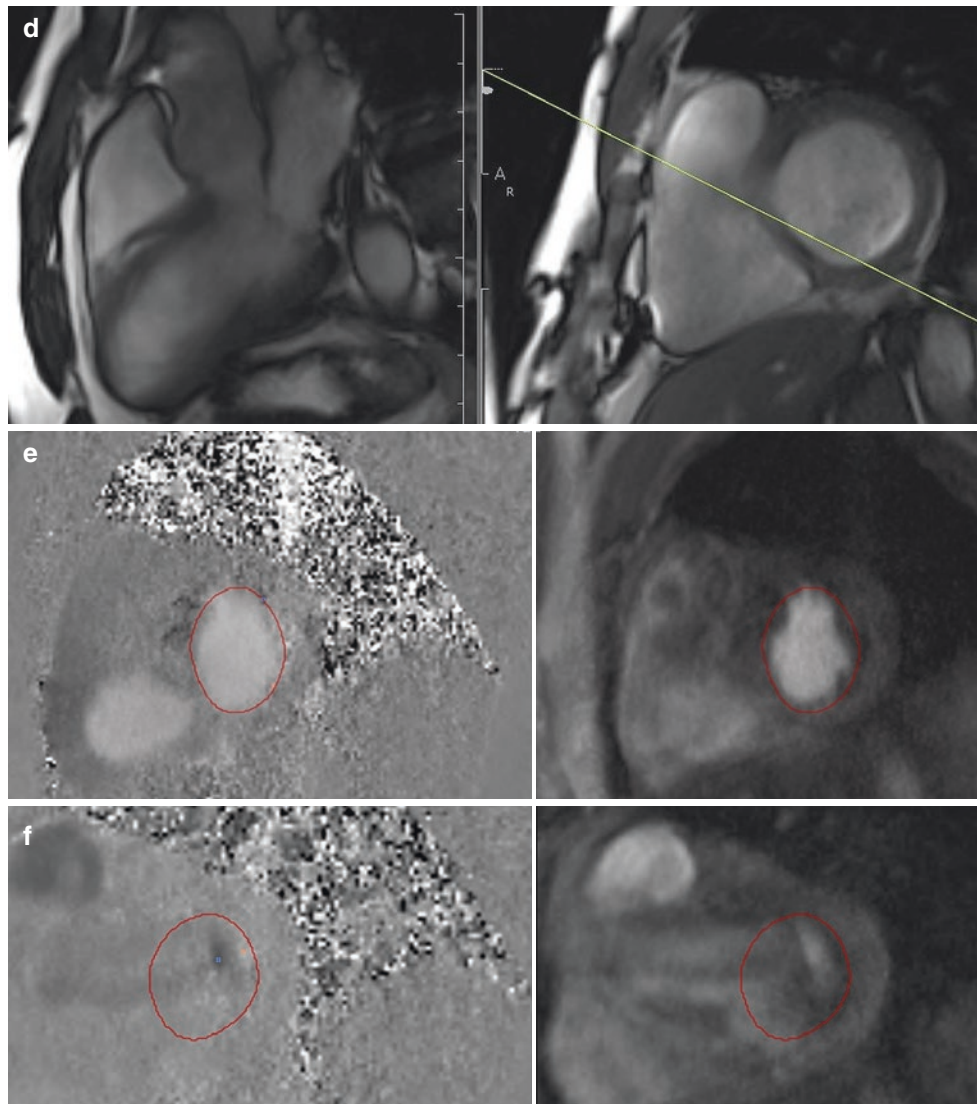


Fig. 18.8 (continued)

of pulmonic velocity can be made by measuring peak velocity with through-plane phase-velocity mapping imaging in similar way to aortic stenosis [1]. Long-axis cine view through the RVOT also enables to assess for supra-valvular or subvalvular pulmonic stenosis. CMR also allows for accurate right ventricular mass and function assessment and determination of hemodynamic effect of pulmonic stenosis [6].

Pulmonary Regurgitation

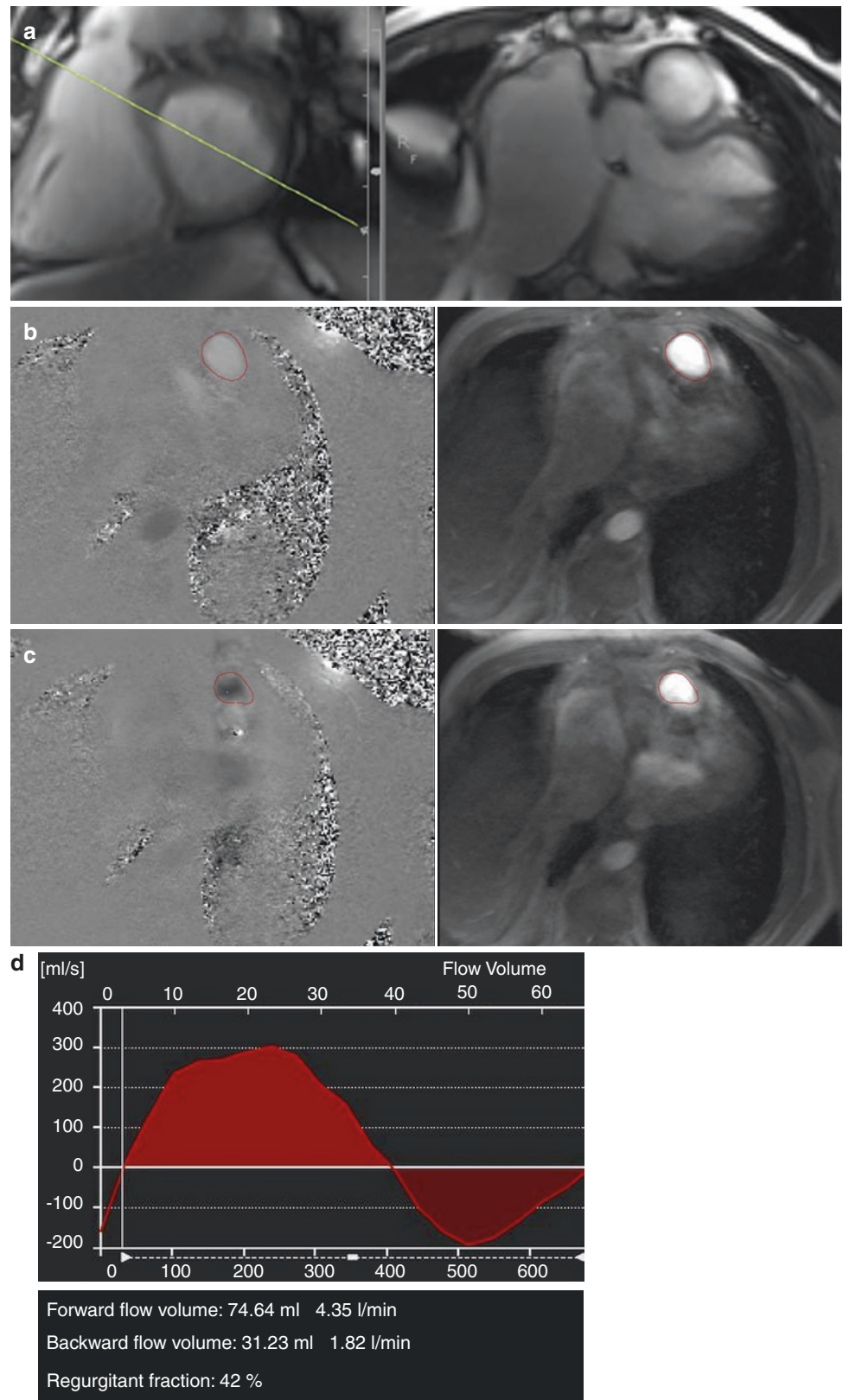
Evaluation of pulmonary regurgitation is especially important in patients with Tetralogy of Fallot whose statuses are post-repair and where accurate estimation of regurgitation

severity and right ventricular volume/function are extremely important [1].

Pulmonary regurgitation can be visualized in the steady-state free-precession cine imaging as a signal void in the RVOT. It should be noted, though, that the degree of turbulence might be lower due to lower pressures and the wide jet of PR with mostly laminar flow on the right side which can make visualization of regurgitation might more difficult [6] (Fig. 18.9).

Hence, the in-plane phase-contrast velocity mapping is usually preferred for visualization of the regurgitant jet [6]. Quantification of regurgitant flow with through-plane velocity mapping is performed on an image slice placed just above the pulmonary valve [1]. On the in-plane velocity mapping,

Fig. 18.9 A 52-year-old male with history of pulmonic stenosis status post-valvulotomy in childhood and now presenting with dyspnea on exertion. **(a)** Sagittal SSFP cine image through the right ventricular outflow tract and pulmonary artery (left) and short-axis SSFP slice below the pulmonic valve (right) for the phase-contrast positioning. **(b)** Magnitude and phase-contrast images below the pulmonic valve in systole. **(c)** Magnitude and phase-contrast images below the pulmonic valve in diastole showing pulmonic regurgitation in black which calculated to be moderate to severe. **(d)** Corresponding plots of velocity vs time-volume curve showing antegrade and retrograde flow with resultant regurgitation fraction of 42%=severe pulmonary regurgitation



the wide regurgitant jet is clearly seen in as black. Robenberg et al. showed that CMR velocity mapping is an accurate method for the noninvasive, volumetric quantification of pulmonary regurgitation after surgical correction of tetralogy of Fallot [46]. Mercer-Rosa et al. showed that when comparing echocardiography with CMR in patients with repaired TOF, where regurgitant fraction >40% is considered severe, echocardiography continues to have a limited ability to quantify PR and RV function as compared with CMR [47]. Furthermore, Li et al. showed that when evaluated in adults with repaired tetralogy of Fallot, direct quantification of the pulmonary regurgitation with CMR agrees well with echocardiographic parameters [48]. CMR also can be helpful in determining timing for pulmonary valve replacement as it accurately assesses RV volume and function [49].

Tricuspid Stenosis

Tricuspid stenosis is very rare and is not commonly assessed by CMR. If needed, cine SSFP images can be obtained which easily can visualize the anatomy and function of the leaflets. The tricuspid valve area can be assessed by placing image slice through the valve tips in diastole, in similar way in assessment of mitral stenosis. The forward velocity can also be measured through the valve with phase-velocity imaging as well although it might be less useful [1].

Tricuspid Regurgitation

CMR is particularly useful in assessment of leaflet morphology such as in Ebstein's anomaly [50]. For example, four-chamber SSFP cine image can identify the displacement of the valve or abnormal movement of the leaflets. Due to thin nature of the tricuspid leaflets and limited spatial resolution of CMR, it might be difficult to assess for adherence of the tricuspid leaflets to the myocardium [1]. Qualitatively, the tricuspid regurgitation can be evaluated by in-plane phase imaging in the four-chamber view or in the two-chamber view focusing on the right atrium and the right ventricle. The velocity encoding setting should be around ~150 cm/sec. (Fig. 18.10).

Special Considerations

Prosthetic Valves

Cardiac magnetic resonance (CMR) could be an alternative noninvasive imaging modality that can be utilized to assess prosthetic valve function by direct planimetry of the anatomic orifice area (AOA) and for assessment of peak through-plane velocity by use of phase-contrast (PC) techniques.

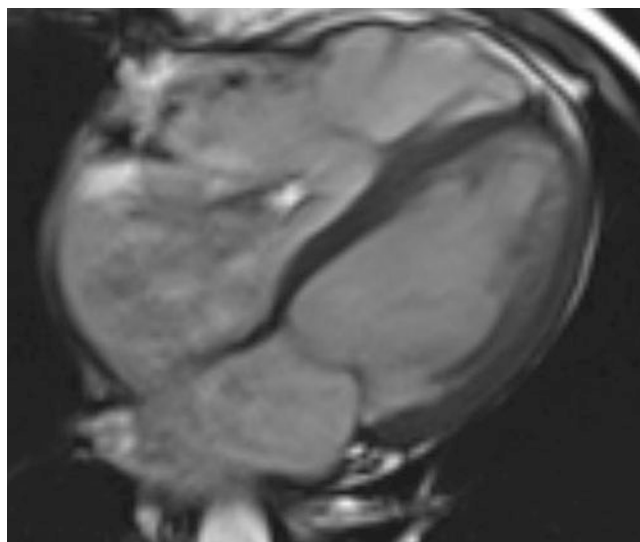


Fig. 18.10 SSFP cine four-chamber image showing severe tricuspid regurgitation with apical displacement of tricuspid septal leaflet in a patient with Ebstein's anomaly. The RA and RV are moderately dilated

Maragiannis et al. showed that estimation of effective orifice area with phase contrast is a feasible, accurate, and reproducible parameter that may be calculated to assess both normal and abnormal bioprosthetic aortic valve functions [51]. Mechanical heart valves often produce complex flow patterns that make precise assessment via Doppler echocardiography challenging. In this respect, CMR can be quite helpful in addition to defining structure, position, and flow across the orifice and associated changes in the valvular apparatus and chambers. However, these valves can induce susceptibility artifacts and often necessitate phase-contrast imaging in particular, to be acquired outside the magnetic field distortion [52]. The SSFP cine sequence is very sensitive to artifacts from ferromagnetic objects which can both arise from both mechanical and bioprosthetic valves. Currently all mechanical valves are considered safe for imaging in a 1.5 Tesla environment because heating and torque due to the magnetic field is considerably small [52, 53], unless if clinical valvular dehiscence is suspected, then CMR imaging may pose additional risk to the patient with an already impaired heart artificial valve.

CMR can also be an alternative method for assessment of new percutaneous valves. Hamilton Craig et al. showed that CMR performs very well in the quantitation of MR after MitraClip insertion, with excellent reproducibility compared to echocardiographic methods [54]. Secchi et al. evaluated patient status post-tetralogy of Fallot repair and showed that CMR demonstrated restored pulmonary conduit function, reduced RV volumes, and increased RV and LV function but did not predict valve fracture/restenosis [50]. Hartlage et al.

showed that CMR more accurately classifies severity of paravalvular aortic regurgitation, providing superior prognostic value compared with echocardiography, as patients with greater than mild paravalvular regurgitation by CMR, defined as regurgitant fraction >20%, had a higher incidence of adverse events [55].

Pre- and Postsurgical Assessment

In pre- and postsurgical assessment, CMR not only provides comprehensive information on valvular and ventricular function, but it may also assist in prognosis of the patient. CMR can also aid in determining the type of surgical procedure and the impact that the procedure holds on cardiac hemodynamics during recovery. Barone-Rochette et al. showed that the presence of LGE indicating focal fibrosis or unrecognized infarct by CMR is an independent predictor of mortality in patients with AS undergoing AVR and could provide additional information in the preoperative evaluation of risk in these patients [25]. CMR is also very useful in presurgical planning and for postsurgical evaluation in congenital patients. Fogel et al. demonstrated that single-ventricle patients not requiring an intervention can undergo successful Fontan completion with CMR and echo alone with similar short-term outcomes to patient who underwent catheterization, which was used as a control, preventing an invasive test and exposure to radiation [56]. Geva et al. evaluated patients with post-tetralogy of Fallot repair and showed that severe RV dilatation and either LV or RV dysfunction assessed by CMR predicted major adverse clinical events in this population [57].

In patients who had received a mechanical valve compared to those with nonmechanical ones, CMR was able to demonstrate a greater decrease in the absolute value of systolic strain [58]. Effects on left ventricular mass among patients with severe aortic stenosis who had undergone stentless versus stented porcine valve replacement can also be compared with some precision with CMR [59]. The extent of left atrial and left ventricular reverse remodeling and impact on absolute left ventricular strain can also be demonstrated by CMR [60]. Tissue-tagging is another useful tool in CMR for comparing the type of prosthetic valve used in aortic valve replacement and its impact on incompletely recovered systolic strain in chronic aortic regurgitation [43, 46]. Moreover, CMR is able to assess surgical approaches to valve sparing with regard to preservation of the native sinuses of Valsalva where it has demonstrated that such aortic vortical blood flow is absent in postoperative patients with Marfan syndrome [61]. The determination of regurgitant fraction, ventricular dimensions and functions, and graft diameters allows standardized imaging protocols with a high reproducibility, which may lead to this technique being favored for

the follow-up of patients after surgery involving the heart valves or the great vessels.

Limitations

Arrhythmias can greatly affect the image quality and can also disrupt accurate ventricular volume acquisition as well as valvular flow assessment [62]. Difficulty with breath-holding may also negatively impact the image. Visual assessment from cine images alone should not be done as turbulent flow can produce signal void which can mimic regurgitation. In some instances, slice orientation may not be placed directly perpendicular to the flow in which case VENC may underestimate velocities. Velocities may be also underestimated due to partial volume averaging. Therefore, careful planning needs to be done for each valvular assessment.

Summary

Cardiovascular magnetic resonance allows for a comprehensive evaluation of simple and complex valvular heart disease. The main advantage of CMR for assessment of valvular heart disease is its true and reproducible measurements of ventricular volumes and function which can guide a clinician regarding appropriate timing of surgery. CMR can also provide quantitative measure of valvular stenosis and regurgitation which is comparable to echocardiography. Currently, studies evaluating clinical outcomes by CMR are being investigated, some of which already have shown that aortic regurgitation fraction of >33%, pulmonary regurgitation fraction of >40%, and mitral regurgitation fraction >50% predict symptom development and the need for valve replacement [1, 30, 62]. Therefore, CMR is an attractive alternative or complimentary modality for thorough assessment of valvular pathology.

References

1. Myerson SG. Heart valve disease: investigation by cardiovascular magnetic resonance. *J Cardiovasc Magn Reson*. 2012;14:7.
2. Cawley PJ, Maki JH, Otto CM. Cardiovascular magnetic resonance imaging for valvular heart disease: technique and validation. *Circulation*. 2009;119(3):468–78.
3. Han Y, Peters DC, Salton CJ, Bzymek D, Nezafat R, Goddu B, et al. Cardiovascular magnetic resonance characterization of mitral valve prolapse. *JACC Cardiovasc Imaging*. 2008;1(3):294–303.
4. Lopez-Mattei JC, Shah DJ. The role of cardiac magnetic resonance in valvular heart disease. *Methodist Debakey Cardiovasc J*. 2013;9(3):142–8.
5. Sommer G, Bremerich J, Lund G. Magnetic resonance imaging in valvular heart disease: clinical application and current role for patient management. *J Magn Reson Imaging*. 2012;35(6):1241–52.

6. Karamitsos TD, Myerson SG. The role of cardiovascular magnetic resonance in the evaluation of valve disease. *Prog Cardiovasc Dis*. 2011;54(3):276–86.
7. Gatehouse PD, Keegan J, Crowe LA, Masood S, Mohiaddin RH, Kreitner KF, et al. Applications of phase-contrast flow and velocity imaging in cardiovascular MRI. *Eur Radiol*. 2005;15(10):2172–84.
8. Kilner PJ, Firmin DN, Rees RS, Martinez J, Pennell DJ, Mohiaddin RH, et al. Valve and great vessel stenosis: assessment with MR jet velocity mapping. *Radiology*. 1991;178(1):229–35.
9. O'Brien KR, Gabriel RS, Greiser A, Cowan BR, Young AA, Kerr AJ. Aortic valve stenotic area calculation from phase contrast cardiovascular magnetic resonance: the importance of short echo time. *J Cardiovasc Magn Reson*. 2009;11:49.
10. Nishimura RA, Otto CM, Bonow RO, Carabello BA, Erwin JP 3rd, Guyton RA, et al. 2014 AHA/ACC guideline for the management of patients with valvular heart disease: a report of the American College of Cardiology/American Heart Association Task Force on Practice Guidelines. *J Thorac Cardiovasc Surg*. 2014;148(1):e1–e132.
11. Bellenger NG, Burgess MI, Ray SG, Lahiri A, Coats AJ, Cleland JG, et al. Comparison of left ventricular ejection fraction and volumes in heart failure by echocardiography, radionuclide ventriculography and cardiovascular magnetic resonance; are they interchangeable? *Eur Heart J*. 2000;21(16):1387–96.
12. Myerson SG, Bellenger NG, Pennell DJ. Assessment of left ventricular mass by cardiovascular magnetic resonance. *Hypertension*. 2002;39(3):750–5.
13. Koch JA, Poll LW, Godehardt E, Korbacher B, Modder U. Right and left ventricular volume measurements in an animal heart model in vitro: first experiences with cardiac MRI at 1.0 T. *Eur Radiol*. 2000;10(3):455–8.
14. Walsh TF, Hundley WG. Assessment of ventricular function with cardiovascular magnetic resonance. *Magn Reson Imaging Clin N Am*. 2007;15(4):487–504. v
15. Pennell DJ. Ventricular volume and mass by CMR. *J Cardiovasc Magn Reson*. 2002;4(4):507–13.
16. Armstrong AC, Gidding S, Gjesdal O, Wu C, Bluemke DA, Lima JA. LV mass assessed by echocardiography and CMR, cardiovascular outcomes, and medical practice. *JACC Cardiovasc Imaging*. 2012;5(8):837–48.
17. John AS, Dill T, Brandt RR, Rau M, Ricken W, Bachmann G, et al. Magnetic resonance to assess the aortic valve area in aortic stenosis: how does it compare to current diagnostic standards? *J Am Coll Cardiol*. 2003;42(3):519–26.
18. Kupfahl C, Honold M, Meinhart G, Vogelsberg H, Wagner A, Mahrholdt H, et al. Evaluation of aortic stenosis by cardiovascular magnetic resonance imaging: comparison with established routine clinical techniques. *Heart*. 2004;90(8):893–901.
19. Kramer CM, Barkhausen J, Flamm SD, Kim RJ, Nagel E. Standardized cardiovascular magnetic resonance imaging (CMR) protocols, society for cardiovascular magnetic resonance: board of trustees task force on standardized protocols. *J Cardiovasc Magn Reson*. 2008;10:35. <https://doi.org/10.1186/1532-429X-10-35>.
20. Caruthers SD, Lin SJ, Brown P, Watkins MP, Williams TA, Lehr KA, et al. Practical value of cardiac magnetic resonance imaging for clinical quantification of aortic valve stenosis: comparison with echocardiography. *Circulation*. 2003;108(18):2236–43.
21. Sondergaard L, Hildebrandt P, Lindvig K, Thomsen C, Stahlberg F, Kassis E, et al. Valve area and cardiac output in aortic stenosis: quantification by magnetic resonance velocity mapping. *Am Heart J*. 1993;126(5):1156–64.
22. Pouleur AC, le Polain de Waroux JB, Pasquet A, Vancraeynest D, Vanoverschelde JL, Gerber BL. Planimetric and continuity equation assessment of aortic valve area: head to head comparison between cardiac magnetic resonance and echocardiography. *J Magn Reson Imaging*. 2007;26(6):1436–43.
23. Mohiaddin RH, Kilner PJ. Valvular heart disease. In: Manning WJ, Pennell DJ, editors. *Cardiovascular magnetic resonance*. Philadelphia: Churchill Livingstone; 2002. p. 387–404.
24. O'Brien KR, Gabriel RS, Greiser A, Cowan BR, Young AA, Kerr AJ. Aortic valve stenotic area calculation from phase contrast cardiovascular magnetic resonance: the importance of short echo time. *J Cardiovasc Magn Reson*. 2009;11:49.
25. Barone-Rochette G, Pierard S, De Meester de Ravenstein C, Seldrum S, Melchior J, Maes F, et al. Prognostic significance of LGE by CMR in aortic stenosis patients undergoing valve replacement. *J Am Coll Cardiol*. 2014;64(2):144–54.
26. Wagner S, Auffermann W, Buser P, Lim TH, Kircher B, Pflugfelder P, Higgins CB. Diagnostic accuracy and estimation of the severity of valvular regurgitation from the signal void on cine magnetic resonance images. *Am Heart J*. 1989;118:760–7.
27. Dyverfeldt P, Bissell M, Barker AJ, Bolger AF, Carlhall CJ, Ebbens T, et al. 4D flow cardiovascular magnetic resonance consensus statement. *J Cardiovasc Magn Reson*. 2015;17(1):72.
28. Keegan J, Gatehouse PD, John AS, Mohiaddin RH, Firmin DN. Breath-hold signal-loss sequence for the qualitative assessment of flow disturbances in cardiovascular MR. *J Magn Reson Imaging*. 2003;18(4):496–501.
29. Nishimura T, Yamada N, Itoh A, Miyatake K. Cine MR imaging in mitral regurgitation: comparison with color Doppler flow imaging. *AJR Am J Roentgenol*. 1989;153:721–4.
30. Myerson SG, d'Arcy J, Mohiaddin R, Greenwood JP, Karamitsos TD, Francis JM, et al. Aortic regurgitation quantification using cardiovascular magnetic resonance: association with clinical outcome. *Circulation*. 2012;126(12):1452–60.
31. Sondergaard L, Lindvig K, Hildebrandt P, Thomsen C, Stahlberg F, Joen T, et al. Quantification of aortic regurgitation by magnetic resonance velocity mapping. *Am Heart J*. 1993;125(4):1081–90.
32. Suzuki JI, Caputo GR, Kondo C, Higgins CB. Cine MR imaging of valvular heart disease: display and imaging parameters affect the size of the signal void caused by valvular regurgitation. *AJR Am J Roentgenol*. 1990;155:723–7.
33. Sechtem U, Pflugfelder PW, Cassidy MM, White RD, Cheitlin MD, et al. Mitral or aortic regurgitation: quantification of regurgitant volumes with cine MR imaging. *Radiology*. 1988;167(2):425–30.
34. Baldy C, Douek P, Croisille P, Magnin IE, Revel D, Amiel M. Automated myocardial edge detection from breath-hold cine-MR images: evaluation of left ventricular volumes and mass. *Magn Reson Imaging*. 1994;12(4):589–98.
35. Chatzimavroudis GP, Oshinski JN, Franch RH, Pettigrew RI, Walker PG, Yoganathan AP. Quantification of the aortic regurgitant volume with magnetic resonance phase velocity mapping: a clinical investigation of the importance of imaging slice location. *J Heart Valve Dis*. 1998;7(1):94–101.
36. Djavidani B, Debl K, Lenhart M, Seitz J, Paetzel C, Schmid FX, et al. Planimetry of mitral valve stenosis by magnetic resonance imaging. *J Am Coll Cardiol*. 2005;45(12):2048–53.
37. Heidenreich PA, Steffens J, Fujita N, O'Sullivan M, Caputo GR, Foster E, et al. Evaluation of mitral stenosis with velocity-encoded cine-magnetic resonance imaging. *Am J Cardiol*. 1995;75(5):365–9.
38. Lin SJ, Brown PA, Watkins MP, Williams TA, Lehr KA, Liu W, et al. Quantification of stenotic mitral valve area with magnetic resonance imaging and comparison with Doppler ultrasound. *J Am Coll Cardiol*. 2004;44(1):133–7.
39. Ohyama H, Hosomi N, Takahashi T, Mizushige K, Osaka K, Kohno M, et al. Comparison of magnetic resonance imaging and transesophageal echocardiography in detection of thrombus in the left atrial appendage. *Stroke*. 2003;34(10):2436–9.

40. Chan KM, Wage R, Symmonds K, Rahman-Haley S, Mohiaddin RH, Firmin DN, et al. Towards comprehensive assessment of mitral regurgitation using cardiovascular magnetic resonance. *J Cardiovasc Magn Reson*. 2008;10:61.
41. Stork A, Franzen O, Ruschewski H, Detter C, Mullerleile K, Bansmann PM, et al. Assessment of functional anatomy of the mitral valve in patients with mitral regurgitation with cine magnetic resonance imaging: comparison with transesophageal echocardiography and surgical results. *Eur Radiol*. 2007;17(12):3189–98.
42. Gelfand EV, Hughes S, Hauser TH, Yeon SB, Goepfert L, Kissinger KV, et al. Severity of mitral and aortic regurgitation as assessed by cardiovascular magnetic resonance: optimizing correlation with Doppler echocardiography. *J Cardiovasc Magn Reson*. 2006;8(3):503–7.
43. Benjamin J, Pomerantz, Marc D. Krock, Jason R. Wollmuth, Brian P. Cupps, Nicholas T. Kouchoukos, Victor G. Davila-Roman, Michael K. Pasque. Aortic Valve Replacement for Aortic Insufficiency: Valve Type as a Determinant of Systolic Strain Recovery. *J Cardiac Surg*. 2005;20(6):524–9.
44. Uretsky S, Gillam L, Lang R, Chaudhry FA, Argulian E, Supariwala A, et al. Discordance between echocardiography and MRI in the assessment of mitral regurgitation severity: a prospective multicenter trial. *J Am Coll Cardiol*. 2015;65(11):1078–88.
45. Morello A, Gelfand EV. Cardiovascular magnetic resonance imaging for valvular heart disease. *Curr Heart Fail Rep*. 2009;6(3):160–6.
46. Rebergen SA, Chin JG, Ottenkamp J, van der Wall EE, de Roos A. Pulmonary regurgitation in the late postoperative follow-up of tetralogy of Fallot. Volumetric quantitation by nuclear magnetic resonance velocity mapping. *Circulation*. 1993;88(5 Pt 1):2257–66.
47. Mercer-Rosa L, Yang W, Kutty S, Rychik J, Fogel M, Goldmuntz E. Quantifying pulmonary regurgitation and right ventricular function in surgically repaired tetralogy of Fallot: a comparative analysis of echocardiography and magnetic resonance imaging. *Circ Cardiovasc Imaging*. 2012;5(5):637–43.
48. Li W, Davlourous PA, Kilner PJ, Pennell DJ, Gibson D, Henein MY, et al. Doppler-echocardiographic assessment of pulmonary regurgitation in adults with repaired tetralogy of Fallot: comparison with cardiovascular magnetic resonance imaging. *Am Heart J*. 2004;147(1):165–72.
49. Geva T. Indications and timing of pulmonary valve replacement after tetralogy of fallot repair. *Semin Thorac Cardiovasc Surg Pediatr Card Surg Annu*. 2006:11–22.
50. Secchi F, Resta EC, Cannao PM, Tresoldi S, Butera G, Carminati M, et al. Four-year cardiac magnetic resonance (CMR) follow-up of patients treated with percutaneous pulmonary valve stent implantation. *Eur Radiol*. 2015;25(12):3606–13.
51. Maragiannis D, Jackson MS, Flores-Arredondo JH, Autry K, Schutt RC, Alvarez PA, et al. Functional assessment of bioprosthetic aortic valves by CMR. *JACC Cardiovasc Imaging*. 2016 Jul;9(7):785–93.
52. Edwards MB, Taylor KM, Shellock FG. Prosthetic heart valves: evaluation of magnetic field interactions, heating, and artifacts at 1.5 T. *J Magn Reson Imaging*. 2000;12(2):363–9.
53. Edwards MB, Draper ER, Hand JW, Taylor KM, Young IR. Mechanical testing of human cardiac tissue: some implications for MRI safety. *J Cardiovasc Magn Reson*. 2005;7(5):835–40.
54. Hamilton-Craig C, Strugnell W, Gaikwad N, Ischenko M, Speranza V, Chan J, et al. Quantitation of mitral regurgitation after percutaneous MitraClip repair: comparison of Doppler echocardiography and cardiac magnetic resonance imaging. *Ann Cardiothorac Surg*. 2015;4(4):341–51.
55. Hartlage GR, Babaliaros VC, Thourani VH, Hayek S, Chrysohoou C, Ghasemzadeh N, et al. The role of cardiovascular magnetic resonance in stratifying paravalvular leak severity after transcatheter aortic valve replacement: an observational outcome study. *J Cardiovasc Magn Reson*. 2014;16:93.
56. Fogel MA, Pawlowski TW, Whitehead KK, Harris MA, Keller MS, Glatz AC, et al. Cardiac magnetic resonance and the need for routine cardiac catheterization in single ventricle patients prior to Fontan: a comparison of 3 groups: pre-Fontan CMR versus cath evaluation. *J Am Coll Cardiol*. 2012;60(12):1094–102.
57. Geva T. Repaired tetralogy of Fallot: the roles of cardiovascular magnetic resonance in evaluating pathophysiology and for pulmonary valve replacement decision support. *J Cardiovasc Magn Reson*. 2011;13:9.
58. Pomerantz BJ, Krock MD, Wollmuth JR, Cupps BP, Kouchoukos NT, et al. Aortic valve replacement for aortic insufficiency: valve type as a determinant of systolic strain recovery. *J Card Surg*. 2005;20(6):524–9.
59. Perez de Arenaza D, Lees B, Flather M, Nugara F, Husebye T, Jasinski M, et al. ASSERT (Aortic Stentless versus Stented valve assessed by Echocardiography Randomized Trial) investigators. Randomized comparison of stentless versus stented valves for aortic stenosis: effects on left ventricular mass. *Circulation*. 2005;112(17):2696–702.
60. Westenberg JJ, van der Geest RJ, Lamb HJ, Versteegh MI, Braun J, Doornbos J, et al. MRI to evaluate left atrial and ventricular reverse remodeling after restrictive mitral annuloplasty in dilated cardiomyopathy. *Circulation*. 2005;112(9 Suppl):I 437–442.
61. Kvitting JP, Ebbers T, Wigstrom L, Engvall J, Olin CL, Bolger AF. Flow patterns in the aortic root and the aorta studied with time-resolved, 3-dimensional, phase-contrast magnetic resonance imaging: implications for aortic valve-sparing surgery. *J Thorac Cardiovasc Surg*. 2004;127(6):1602–7.
62. Myerson SG, Francis JM, Neubauer S. Direct and indirect quantification of mitral regurgitation with cardiovascular magnetic resonance, and the effect of heart rate variability. *MAGMA*. 2010;23(4):243–9.